

## THE MASS AND HALO DISPERSION PROFILE OF M32

RICHARD NOLTHENIUS

Steward Observatory, University of Arizona, and University of California, Los Angeles

AND

HOLLAND FORD

Space Telescope Science Institute

Received 1985 August 20; accepted 1985 December 11

### ABSTRACT

We present radial velocities of 15 planetary nebulae in the halo of M32 and use them to put constraints on the form of the stellar orbits and on the mass. We have developed a technique to test the compatibility of our velocities with trial velocity dispersion profiles and have here used the models of Jaffe and Merritt with varying amounts of anisotropy. Assuming constant  $M/L$  with radius, our data favor an isotropic dispersion tensor in the halo. The resulting mass is  $7.0 \times 10^8 M_{\odot}$  for a Jaffe model galaxy and  $9.4 \times 10^8 M_{\odot}$  for a de Vaucouleurs model. These correspond to  $M/L_B$  values of 2.8 and 3.7, respectively. Our data indicate that a significantly increasing  $M/L$  with radius is likely only if the stars are on highly radial orbits.

*Subject headings:* galaxies: individual — galaxies: internal motions — galaxies: Local Group — galaxies: structure — nebulae: planetary — radial velocities

### I. INTRODUCTION

In the past decade advances in instrumentation and computer techniques have led to the first velocity measurements of test particles in distant stellar systems (van den Bergh 1969; Huchra, Stauffer, and van Speybroeck 1982; Hesser, Harris, and van den Bergh 1984; Gunn and Griffin 1979; Lupton, Gunn, and Griffin 1984). The new multiple image spectrographs which are just coming into use will provide data on many more objects.

These observations contain dynamical information on the outer regions of such systems, just where integrated light spectra become too noisy to study. To date, most workers have used test particle data to find only a rough rotation rate, an overall velocity dispersion, and an approximate mass from the virial or projected mass estimators. When only 5–10 velocities are available, it is indeed hard to justify anything fancier. With a hundred or more velocities it becomes possible to bin the data in radius and begin to say something about the run of dispersion and rotation with radius. The best example of this is the excellent analysis of the globular cluster M3 by Gunn and Griffin (1979).

For sample sizes of 15–50 the situation is more awkward; binning reduces the sample sizes to the point that little can be said. A better way would test dispersion profiles against the unbinned data. The problem is that a straightforward unbinned dispersion contains no information about the trends with radius which distinguish between profiles. Fortunately, systems bright enough to have detectable test particles will often have nuclear velocity dispersions available. This provides a spatial baseline extending from the nucleus to the regions containing the test particles. In this paper we present a method of testing trial dispersion profiles based on this idea and apply it to the planetary nebula velocities in M32.

### II. OBSERVATIONS

#### a) *Identifications*

M32 projects onto the disk of M31 at a point  $\sim 13$  kpc from the nucleus. It is therefore important to identify which planet-

aries go with which galaxy. Fortunately, the velocity separation between the two is large. Assuming a rotation speed of  $232 \text{ km s}^{-1}$  and a systemic velocity of  $-305 \text{ km s}^{-1}$  for M31, the disk at M32's position has a line-of-sight velocity of about  $-400 \text{ km s}^{-1}$ . M32's systemic velocity is about  $-185 \text{ km s}^{-1}$ , for a velocity difference of  $215 \text{ km s}^{-1}$ . This is more than 5 times the overall velocity dispersions of the M31 disk and of the M32 planetaries, so there is little danger of assigning M32 planetaries to M31. The reverse is not as clear-cut; the dispersion of the halo M31 planetaries is  $\sim 112 \text{ km s}^{-1}$  (Nolthenius and Ford 1986), about the same as the systemic velocity difference. However, the estimated distribution of M31 halo planetaries yields only  $\sim 0.2$  halo objects in the  $2.8 \text{ kpc}^2$  M32 survey field (Nolthenius and Ford 1986), and the observed velocities do seem to clearly separate the members of the two galaxies.

In a previous paper Ford and Jenner (1975) identified 21 possible planetary nebulae in M32. Radial velocities showed that three of these nebulae (M32-4, M32-12, and M32-17) are planetaries in M31 which project into the M32 field. Two other nebulae (M32-18 and M32-19) were considered possible members of M31, leaving 16 M32 candidates. Eleven of these 16 have radial velocities and line intensities which show that they are planetary nebulae gravitationally bound to M32. Subsequent radial velocity measurements of one of the remaining five (M32-20) showed that it also is a member of the M32 system. The four planetary nebulae without confirming velocity measurements are almost certainly real because they appear on two or more on-band plates or pictures, and are probable members of M32.

Lawrie and Ford used a velocity modulating camera (VMC) to isolate planetary nebulae in the central 250 pc of M31 and M32. By combining the slow  $f/17.5$  Cassegrain focus of the Shane 3 m telescope with a very narrow band ( $1.2 \text{ \AA}$  FWHM) [O III]  $\lambda 5007$  interference filter tuned to M32's systemic velocity, they were able to suppress the light from M32's bright core and detect four nebulae within  $9''$  (30 pc) of M32's nucleus. One of the nebulae, M32-27, projects  $3''.75$  (12 pc) from M32's nucleus. These nebulae, each of which appeared on two VMC

TABLE 1  
PLANETARY NEBULAE IN M32  
WITHOUT RADIAL VELOCITIES

Nebula	$r$	$\theta$
9.....	134.6	188.50
10.....	64.3	33.70
21.....	16.0	163.94
22.....	101.1	115.78
24.....	6.5	89.34
27.....	3.6	14.56
28.....	20.7	158.15

on-band planets, were confirmed by a pair of videocamera on-band (5010/23) and off-band (5300/200) pictures taken with the Mayall 4 m telescope (see Ford 1983 for a finding chart), and by spectrophotometry of three of the nebulae. The videocamera picture showed two additional nebulae which did not appear in the VMC pictures. One of these, M32-24, is almost certainly real and probably has a velocity which falls outside the 2.1 Å FWHM ( $125 \text{ km s}^{-1}$  FWHM) bandpass of the VMC plates. The second, M32-28, although very faint, is a plausible

candidate. Table 1 lists the probable members of M32 which do not have confirming radial velocities. In Table 2 we list the certain members of M32. The first column gives the designations of the nebulae; the second and third columns list their radii and position angles relative to the nucleus ( $\alpha_{1950} = 00^{\text{h}}41^{\text{m}}19^{\text{s}}.67$ ,  $\delta_{1950} = 40^{\circ}43'41''.5$ ). The fourth and fifth columns, respectively, list the Lick image tube scanner (ITS) and Kitt Peak intensified image dissector scanner (IIDS) heliocentric radial velocities. The last column gives the correction due to rotation, discussed in § IIIa. The radial velocities are discussed in the following section. Planetary nebulae which are probably not members of M32 but project into the M32 field are listed in Table 3.

### b) Radial Velocities

#### i) Lick ITS Velocities

The Lick ITS velocities were measured at H $\alpha$  with a 1200 l  $\text{mm}^{-1}$  grating used in the first order, giving a reciprocal dispersion of  $73 \text{ \AA mm}^{-1}$ , or  $0.63 \text{ \AA}$  per channel (see Ford and Jenner 1975; Ford, Jacoby, and Jenner 1978). We used two independent reductions of the data to measure radial velocities

TABLE 2  
RADIAL VELOCITIES OF PLANETARY NEBULAE IN M32

NEBULA	DATE OBSERVED	$r$	P.A.	$V_0$		$\langle v_0 \rangle$	$v_r$
				Lick ITS	KPNO IIDS		
1.....	1974 Aug 20	94.4	314.4	-202	...	...	...
	1974 Sep 16	...	...	-179	...	...	...
	1974 Sep 17	...	...	-196	...	...	...
	1974 Oct 12	...	...	-201	...	...	...
	1974 Oct 13	...	...	-190	...	...	...
	1977 Oct 06	...	...	...	-191	-193	-15
2.....	1974 Oct 13	215.8	143.9	-210	...	-210	11
3.....	1974 Aug 21	55.3	199.7	-134	...	-134	17
5.....	1974 Sep 16	52.4	330.9	-211	...	...	...
	1974 Oct 14	...	...	-228	...	...	...
	1977 Oct 06	...	...	...	-248	-229	-22
6.....	1974 Sep 16	51.9	341.0	-187	...	...	...
	1977 Oct 06	...	...	...	-203	-195	-23
7.....	1974 Sep 17	156.4	27.4	-159	...	...	...
	1974 Sep 18	...	...	-188	...	-174	-9
8.....	1974 Aug 20	270.9	122.0	-156	...	...	...
	1974 Oct 12	...	...	-139	...	-147	8
11.....	1974 Oct 13	179.7	107.0	-175	...	...	...
	1974 Oct 06	...	...	...	-183	-179	7
13.....	1974 Aug 21	228.3	172.3	-181	...	-181	11
14.....	1974 Aug 21	57.4	198.5	-154	...	-154	17
15.....	1974 Aug 21	66.1	246.7	-241	...	...	...
	1974 Oct 13	...	...	-262	...	...	...
	1974 Oct 14	...	...	-280	...	-261	1
20.....	1977 Oct 06	23.4	184.7	...	-212	-212	31
23.....	1977 Oct 06	7.7	139.2	...	-253	-253	54
25.....	1977 Oct 06	8.8	81.5	...	-156	-156	11
26.....	1977 Oct 06	7.9	40.4	...	-242	-242	-29

Col. (3).—Projected radius in arc seconds.

Col. (5).—Lick ITS velocity in  $\text{km s}^{-1}$ .

Col. (6).—Kitt Peak IIDS velocity corrected to Lick system, in  $\text{km s}^{-1}$ .

Col. (7).—Final adopted velocity is the mean of all velocities, in  $\text{km s}^{-1}$ .

Col. (8).—Rotation component; to be subtracted from col. (7) to get nonrotating velocities, in  $\text{km s}^{-1}$ .

TABLE 3  
PROBABLE NONMEMBER PLANETARIES PROJECTED IN M32 FIELD

Nebula	R.A. (1975.0)	decl. (1975.0)	$r$	P.A.	KPNO $v_0$ ( $\text{km s}^{-1}$ )
4.....	0 <sup>h</sup> 41 <sup>m</sup> 08 <sup>s</sup> .91	+40°44'51".9	142.9	330.8	-425.4
12.....	0 41 32.37	40 43 54.4	142.5	85.1	-664
17.....	0 41 04.82	40 41 28.9	216.9	217.8	-428
18.....	0 41 09.27	40 45 10.0	149.2	306.1	...
19.....	0 41 14.7	40 41 49.9	145.6	203.8	...

Col. (4).—Projected radius from M32 nucleus in arc seconds. Planetary M32-18 and M32-19 are only identified on one plate, and may have velocities beyond the window for the H $\alpha$  and [O III]  $\lambda$ 5007 plates. If so they are probably members of M31. See Ford and Jenner 1975.

from [N II]  $\lambda$ 6548, H $\alpha$ , and [N II]  $\lambda$ 6584. In the first procedure, neon comparison spectra taken immediately before and after the observations of a planetary were summed, and a cubic polynomial was fitted to five lines between 6334 and 6717 which bracket [N II] and H $\alpha$ . The positions of the planetary's lines were measured manually by using a cursor to bisect an expanded display of the [N II] and H $\alpha$  lines. In the second procedure a cubic polynomial was fitted to 11 neon lines between 6217 and 6717, in the "before" and "after" comparison spectrum sum. The spectrum was then linearized, and the positions of the airglow lines [O I]  $\lambda$ 6300/ $\lambda$ 6360, and the [N II] and H $\alpha$  lines were measured by an automatic line identification and centering algorithm. The procedures are in excellent agreement, with a mean difference of  $1 \text{ km s}^{-1}$  for 19 velocity pairs and a dispersion of  $14 \text{ km s}^{-1}$  around the mean. Consequently, in order to reduce accidental errors with either procedure, we averaged the velocities derived from the two methods. These velocities are given in Table 2.

Two facts suggest that systematic errors in the [N II] and H $\alpha$  velocities are small. First, 212 measurements of the airglow [O I]  $\lambda$ 6300/ $\lambda$ 6360 radial velocities in the linearized spectra gave a mean velocity of  $4.6 \text{ km s}^{-1}$  with a dispersion of  $17 \text{ km s}^{-1}$ . Second, the ITS radial velocities for two semistellar galactic planetary nebulae, M1-2 and VY2-3, which are discussed by Ford, Jacoby, and Jenner (1977) showed that the velocity corrections to H $\alpha$  are  $|\Delta_{\text{cor}}| \leq 6 \text{ km s}^{-1}$ . Consequently, we have not applied a velocity correction to the [N II] and H $\alpha$  velocities.

The random errors in the ITS velocities can be estimated from those nebulae which have more than one velocity measurement. Five radial velocity measurements of M32-1, one of the brightest planetaries in M32, give a  $9 \text{ km s}^{-1}$  dispersion about the mean. The average standard deviation for the six nebulae with two or more radial velocity measurements is  $12.6 \text{ km s}^{-1}$ . We will adopt this value for the measurement error  $\sigma_e$ , and conservatively estimate that the errors are typically no worse than  $15 \text{ km s}^{-1}$ .

#### ii) Kitt Peak IIDS Radial Velocities

Eight planetary nebulae, including four near the nucleus, were observed at H $\beta$  and [O III]  $\lambda$  $\lambda$ 4959, 5007 with the IIDS and "gold" spectrograph on the Mayall 4 m telescope. The observations were made with a 81 mm aperture and an 830  $l \text{ mm}^{-1}$  grating used in the second order, which gave a reciprocal dispersion of  $34 \text{ \AA mm}^{-1}$ , or  $0.68 \text{ \AA}$  per channel. Because of the difficulty of centering the nebulae for maximum signal when working in M32's bright core, the nebulae were observed in the east aperture only. The bright continuum from starlight

in M32 was flattened by dividing the east spectrum by the spectrum from the west aperture. A quadratic polynomial was fitted to five helium and argon lines between 4880 and 5048  $\text{\AA}$  in the comparison spectrum taken immediately after the observations. The centers of the planetary emission lines were measured by visual bisection on an expanded display of the spectrum.

Radial velocity observations of the semistellar galactic planetaries VY 2-3 ( $V_0 = -43.5 \text{ km s}^{-1}$ ; Ford, Jacoby, and Jenner 1977) and M1-2 ( $V_0 = -17.6 \text{ km s}^{-1}$ ; O'Dell 1966) were used to put the Kitt Peak velocities into the same system as the Lick velocities. Schneider *et al.* (1983) have published new velocities for VY 2-3 ( $V_0 = -49.6 \text{ km s}^{-1}$ ) and for M1-2 ( $V_0 = -10.7 \text{ km s}^{-1}$ ). When we consider all of our Lick ITS and Kitt Peak IIDS observations of VY 2-3 and M1-2, it is clear that the difference in velocities between the two nebulae is approximately  $-32 \text{ km s}^{-1}$  when measured by the Balmer lines, whereas the velocity difference measured with the [O III]  $\lambda$  $\lambda$ 4959, 5007 lines is  $-23 \text{ km s}^{-1}$ . The latter value is much more consistent with our adopted velocities ( $\Delta V = -25.9 \text{ km s}^{-1}$ ) than with the Schneider *et al.* velocities ( $\Delta V = -38.9 \text{ km s}^{-1}$ ). Because we primarily rely on [O III]  $\lambda$  $\lambda$ 4959, 5007 for the IIDS velocity measurements of these high-excitation nebulae, we will use our adopted velocities for VY 2-3 and M1-2 to correct the Kitt Peak velocities to the Lick system.

The average velocity correction required to force the H $\beta$  velocities to the adopted velocities ( $-43.5$  and  $-17.6 \text{ km s}^{-1}$ ), is  $4.4 \pm 2.4 \text{ km s}^{-1}$ . Because the correction factor is small and there is uncertainty about H $\beta$  velocities relative to [O III]  $\lambda$  $\lambda$ 4959, 5007, we did not use the H $\beta$  correction. In any case, because H $\beta$  is a weak line and often undetected or given zero weight, the H $\beta$  correction scheme does not affect the velocities. The [O III] velocities which went into the IIDS velocities in Table 1 have been corrected by adding  $11.2 \text{ km s}^{-1}$  to the observed heliocentric velocities. The mean velocity difference between the four nebulae in Table 1 with both ITS and IIDS velocities is  $12 \text{ km s}^{-1}$  with a dispersion of  $13 \text{ km s}^{-1}$ , which is satisfactory agreement.

### III. ANALYSIS

Given a nuclear dispersion and 15 line of sight velocities at various projected sky positions through the bulk of the galaxy, how might one judge the suitability of a proposed dispersion profile? Combining the velocities into a straightforward dispersion and comparing this to the nuclear value is not efficient, since each planetary nebula samples a different underlying dispersion. One might consider each  $|v|$  as an estimate of the local dispersion (from a sample of size one), and test trial profiles by regression methods. However,  $|v| - \sigma$  does not possess a simple distribution, and confidence limits must be found by Monte Carlo methods. If a nuclear dispersion is not available, this approach may yet be the only choice. It does have the advantage that no assumption need be made that the core and halo can be described by the same model. For small samples such as ours, however, it is doubtful that this method is a significantly better discriminator than the simple approach we prefer. Our method makes no attempt to look for trends with radius in the velocity data alone. Instead, the trend information comes from comparing a combined measure of the planetary nebulae velocity dispersion with the observed nuclear dispersion. We scaled each trial profile, so that when properly convolved with seeing and slit size it produces the observed nuclear dispersion. It then remains to quantify how well the

planetary nebula velocities agree with the rest of the profile. If the planetaries are an unbiased sample of the underlying stellar dispersion, then the expectation of each  $v^2$ , normalized by the sum of the squared trial dispersion at that radius and the error variance, is just one. A convenient goodness of fit test is then how close the sum of squares of these normalized velocities is to the number of degrees of freedom.

This method can be applied to any proposed dispersion profile. Recent models of spherical systems are those of Jaffe (1983), Tonry (1983), Richstone and Tremaine (1984), Newton and Binney (1984), and Merritt (1985).

In Table 4 we list the parameters for M32 in the analysis to follow.

#### a) Model Galaxies

There is no evidence that the radial properties of ellipticals are significantly affected by mildly nonspherical potentials (Saaf 1968). We therefore consider spherical models, neglecting M32's small eccentricity ( $b/a = 0.85$ ; Sharov and Lyutuj 1983). Rotation is more problematic. Tonry has shown that the inner regions of M32 rotate significantly, with projected axis near the photometric minor axis. However, for every rotating model, there is a nonrotating model with the same bulk properties, obtained by simply reversing the direction of some of the orbits. To first order, then, we can fit M32's observed velocities, including the rotational component, to nonrotating models, being careful, however, to consider the rotational components when finding the systemic velocity.

The existence of a density singularity sharper than that for the  $r^{1/4}$  law in the core of M32 is unsettled (Tonry 1984). We test here models with and without such a singularity. Among spherical nonrotating equilibrium models we have chosen two for their simplicity and theoretical plausibility. Jaffe's (1983) model has a brightness profile which agrees with observations as well or better than the de Vaucouleurs  $r^{1/4}$  law, and has a brightness excess at the core, like that claimed by some observers (e.g., Schneider, in Tonry 1984). It also has simple analytic relations for the surface density, space density, and distribution function. We consider its simplest solutions, with anisotropy constant with radius. Some galaxy formation scenarios, however, predict varying anisotropy, e.g., isotropic cores and more radial orbits in the halo. Merritt (1985) has recently generalized Eddington's inversion technique to produce analytically realistic distribution functions from arbitrary spherical mass distributions. His dispersion profiles vary smoothly from an isotropic core to an increasingly anisotropic halo. Here we have used his profiles for the  $r^{1/4}$  law, which

follow Binney (1980), and refer to them as the (anisotropic) de Vaucouleurs models.

#### b) Testing Goodness of Fit

Tonry's Figures 1*b* and 2*b* show the dispersion sharply peaking in the center at 85–95 km s<sup>-1</sup>. His rotation velocity in the core is not well resolved, but appears to be large enough to account for most of the peak (private communication). Whitmore (1980) used a wider slit, obtaining a  $\sigma_{\text{nuc}}$  of 75 km s<sup>-1</sup>, consistent with Tonry's. We have used Whitmore's results as a fiducial value since they represent an average over more of the core and show in § IV how our results vary with assumed nuclear dispersion.

Convolving Merritt's profiles and our Figure 1 profiles with Whitmore's 3" seeing disk and 3" slit and equating the result with 75 km s<sup>-1</sup> gives the scale  $\sigma_0$  for each profile. It also determines the mass of the model, since

$$\sigma_0^2 = \frac{GM}{x}, \quad (1)$$

where  $x = r_e$ , the effective radius for the de Vaucouleurs models, and  $x = r_0$  for the Jaffe models. The quantity  $r_0$  is the (space) radius containing half the luminosity and is  $1.31r_e$  for the Jaffe models. Let the adopted planetary nebula velocity  $v_i$  be the mean of the  $n_i$  observations of that planetary. The rotation component is

$$v_{ri} = v_r(a_i) \cos(\phi_i - \phi_0). \quad (2)$$

The rotation term is a fit to Tonry's (1984) Figures 1*a* and 2*a*, with  $\phi_0 = 69^\circ$ . It is listed in Table 2 as  $v_r$ .

Now form the sum over the  $N$  planetaries:

$$S^2 \equiv \sum_{i=1}^N w_i (v_i - \mu)^2, \quad (3)$$

where the mean systemic velocity  $\mu$  is

$$\mu = \frac{1}{w} \sum_{i=1}^N w_i (v_i - v_{ri}), \quad (4)$$

and the weights  $w_i$  normalize the velocities to the total local dispersion squared:

$$w_i = \frac{1}{\sigma^2(a_i) + (\sigma_e^2/n_i)}. \quad (5)$$

In equation (4) we have used the dot notation to indicate a sum over all planetaries. The weight is thus inversely proportional to the total variance of the observed planetary nebula's velocity. The total variance is just the uncorrelated sum of the intrinsic dispersion  $\sigma_{a_i}$  from the trial profile at the projected separation  $a_i$ , and the measurement uncertainty. This insures a minimum variance estimate of  $\mu$ . If the trial dispersion profile is also the true profile, then the expectation of  $S^2$  is just  $N$  minus the number of degrees of freedom to be fixed. With  $\sigma_0$  set by the nuclear dispersion, there is only one degree of freedom,  $\mu$ , to be fixed by the planetary nebula data. How close  $S^2$  approaches  $N - 1$  is then a measure of the goodness of fit between the observations and the trial dispersion profile. The best-fit profile will be unique, providing the family of profiles considered do not cross outside the imposed intersection at the nucleus. This will be true as long as the corresponding anisotropy profiles likewise do not intersect. The quantity  $S^2$  will then be a monotonic function of anisotropy. The anisotropic

TABLE 4  
ASSUMED PARAMETERS OF M32

Quantity	Value	Source
Distance .....	0.67 Mpc	van den Bergh 1969; Ford, Jacoby, and Jenner 1978
$r^{1/4}$ law effective radius .....	150 pc	de Vaucouleurs 1974
Absolute blue magnitude .....	-15.5	Faber and Jackson 1976
$B - V$ color .....	0.85	de Vaucouleurs, de Vaucouleurs, and Corwin 1976
Nuclear rotation axis P.A. ....	69°	Tonry 1984

de Vaucouleurs models and the Jaffe models with constant anisotropy considered here conform to this condition.

The form of the velocity distribution along the line of sight is not uniquely determined by the density and dispersion profiles. However, if we approximate it as Gaussian,  $S^2$  becomes a sum of squares of unit normal variables and is thus  $\chi^2$  distributed. This allows us to estimate confidence limits on  $S^2$ .

An alternative but more cumbersome test for goodness of fit uses analysis of variance techniques (Nolthenius 1984). Both methods give similar results for M32.

While neither formulation requires that the observed planetaries be distributed like the mass or light, the Kolmogorov-Smirnov test does show that in the sampled range of  $3''$ – $280''$  the planetary nebula distribution does not significantly differ from that of the light.

### c) Scaling

The dispersions  $\sigma(a_i)$  for each planetary can be taken from Figure 1 once the scale  $r_e$  is given. Estimates of  $r_e$  range from  $30''$  (de Vaucouleurs 1953) to  $51''$  (Hubble 1930). As a fiducial value we have used de Vaucouleurs' most recent (1974) value of  $46''$  (150 pc at 0.67 Mpc distance). Fitting the dispersion profiles only requires an angular scale, but the inferred mass is proportional to the distance. We have adopted van den Bergh's (1969) distance to M31 of 0.69 Mpc and assume M32 lies 20 kpc in front of M31 (Ford, Jacoby, and Jenner 1978), for an adopted M32 distance of 0.67 Mpc. At this distance the published values of  $r_e$  range from 97 to 167 pc.

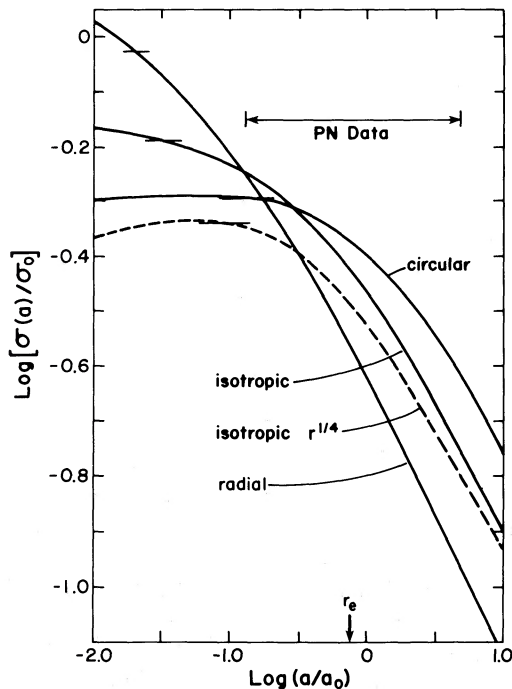


FIG. 1.—Line-of-sight velocity dispersion profiles for the Jaffe circular, isotropic, and radial orbit models (solid) and the isotropic  $r^{1/4}$  law (dashed). Also tested but not shown here were Merritt's (1985)  $r_a = 0.06$  and  $r_a = 0.20$  radial orbit de Vaucouleurs models. Ticks show the seeing convolved, integrated nuclear dispersion. The quantity  $r_e$  is the radius of the sphere containing half the luminosity. Radius range spanned by the planetary nebulae is shown at top.

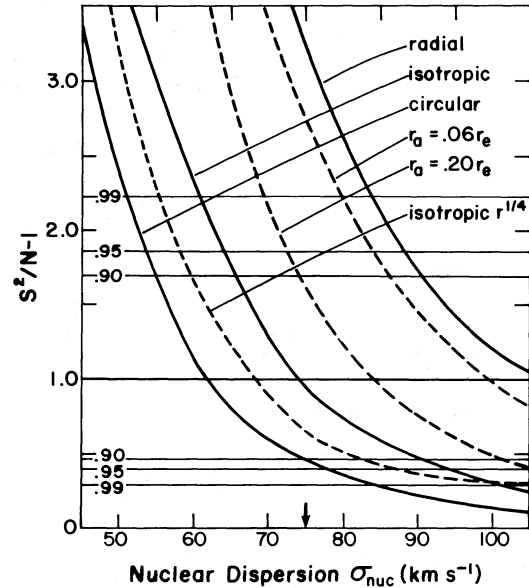


FIG. 2.—The quantity  $S^2$  vs. assumed nuclear velocity dispersion. Jaffe models are solid curves. Anisotropic de Vaucouleurs models are dashed curves. Nuclear dispersions assume  $3''$  seeing and  $3''$  slit width. For  $\sigma_{\text{nuc}}$  near  $65$ – $77$   $\text{km s}^{-1}$ , the isotropic models are favored. Higher  $\sigma_{\text{nuc}}$  favors more radial models. Also shown are 90%, 95%, and 99% confidence ranges, assuming a Gaussian line of sight velocity distribution.

## IV. RESULTS

The overall straightforward dispersion of the planetaries is  $44 \text{ km s}^{-1}$ . Subtracting the observational error of  $12 \text{ km s}^{-1}$  in quadrature gives a rough halo dispersion of  $42 \text{ km s}^{-1}$ . Comparing this to Tonry's  $85$ – $90 \text{ km s}^{-1}$  near the core is strong evidence that the dispersion indeed drops with increasing radius. This also suggests that  $M/L$  does not increase greatly through the bulk of the galaxy outside the nucleus.

The weighted systemic velocity (from eq. [4]) varies slightly between models but is within a couple of  $\text{km s}^{-1}$  of  $-189 \text{ km s}^{-1}$  for all. A straight, unweighted average is  $-199 \text{ km s}^{-1}$ . Tonry's (1984) value is  $-195 \text{ km s}^{-1}$  (private communication).

Figure 2 shows how  $S^2$  varies with assumed nuclear velocity dispersion. These curves use a  $3''$  seeing disk and  $3''$  slit width. The value of  $S^2$  per degree of freedom is near unity for both the isotropic models if the nuclear dispersion is near  $70$ – $75 \text{ km s}^{-1}$ . The confidence limits are rather wide, however. For the  $r^{1/4}$  density law, slightly radial orbits actually fit best.

The dispersion profile fit is much less sensitive to the effective radius, and Figure 3 shows the isotropic or slightly radial models provide good fits through the published range of  $r_e$ . The highly radial models seem unlikely for any reasonable value of  $r_e$ .

Figure 4 shows how  $S^2$  varies with assumed system velocity. The value of  $S^2$  is a minimum at the equation (4) system velocity. This is because the adopted weights guarantee a minimum variance estimate of  $\mu$ . Notice that the highly radial models become even poorer fits away from the systemic velocity given by equation (4).

We have used the results in Figure 3, together with equation (1) and the fact that  $\sigma_0$  is proportional to  $\sigma_{\text{nuc}}$ , to find the range

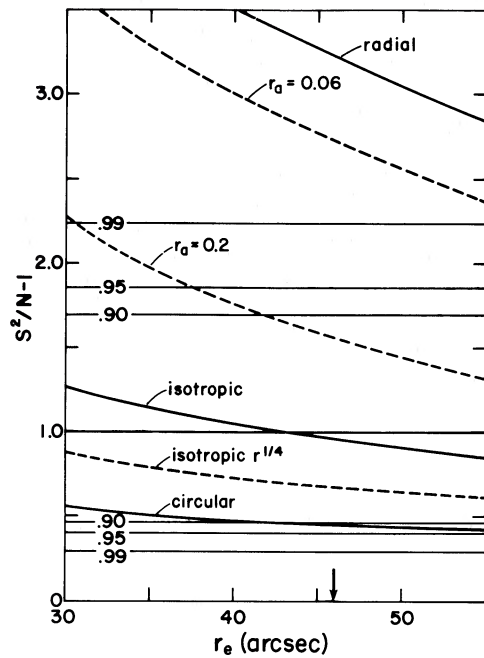


FIG. 3

FIG. 3.—The quantity  $S^2$  vs. assumed effective radius. Fiducial value of  $46''$  is shown with a tick. The quantity  $\sigma_{\text{nuc}}$  is assumed  $66 \text{ km s}^{-1}$ . The quantity  $S^2$  depends only weakly on  $r_e$ , and all reasonable  $r_e$  favor the isotropic models.

FIG. 4.—The quantity  $S^2$  vs. assumed system velocity. Eq. (5) for the isotropic models gives  $-190 \text{ km s}^{-1}$ . Previous published values tend to be lower. The quantity  $\sigma_{\text{nuc}}$  is assumed  $75 \text{ km s}^{-1}$ ;  $r_e = 46''$ . The isotropic models are favored between about  $-175$  and  $-205 \text{ km s}^{-1}$ .

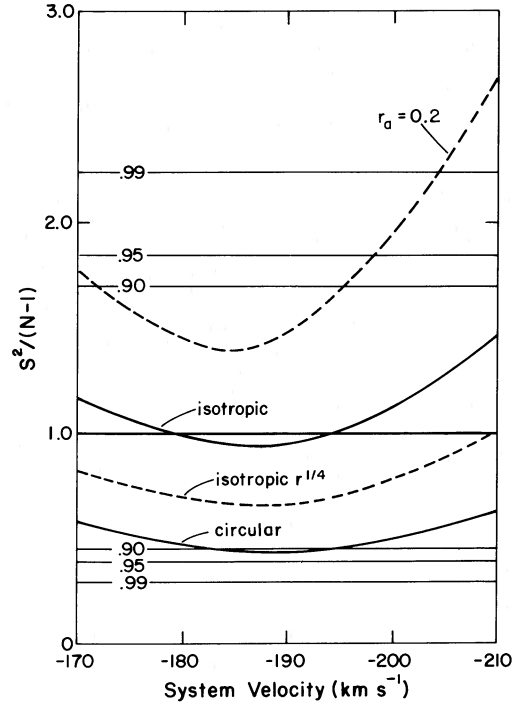


FIG. 4

of acceptable masses for the Jaffe and anisotropic de Vaucouleurs models of M32, shown in Figure 5. The shaded areas make no assumption about the most likely nuclear dispersion. The planetary nebula data favor values near the  $S^2 = N - 1$  curves, subscripted “J” and “M” for Jaffe and Merritt’s de Vaucouleurs models, respectively. In general, the de Vaucouleurs models are 25%–45% more massive than the corresponding Jaffe model at the same  $\sigma_{\text{nuc}}$ . At  $\sigma_{\text{nuc}} = 75 \text{ km s}^{-1}$  the best Jaffe model gives  $7.0 \times 10^8 M_{\odot}$ , and the best de Vaucouleurs model gives  $9.4 \times 10^8 M_{\odot}$ . These correspond to the  $M/L_B$  values of 2.8 and 3.7, respectively, assuming  $M_B = -15.5$  (Faber and Jackson 1976). The dispersion profiles are not physically consistent for Merritt’s de Vaucouleurs models dominated by tangential motion, so we have given no boundary to the left of the isotropic de Vaucouleurs model curve.

The planetary nebula data can also be used to find more conventional mass and  $M/L$  estimates. For comparison we have shown these, as well as recent results from others in Table 5. The projected mass estimator of Heisler, Tremaine, and Bahcall (1985) for distributed masses gives  $8.5 \pm 3 \times 10^8 M_{\odot}$ . The quoted error is the Bahcall and Tremaine (1981) formal error plus 10% to account for uncertainty in the isotropy of the dispersion. A straight number weighted virial mass is  $1.7 \times 10^8 M_{\odot}$ . This estimate is almost certainly too low, since 70% of the mean reciprocal radius is due to the inner three planetaries, which happen to have only moderate velocities. This is an example of inefficiency in the virial mass, pointed out by Bahcall and Tremaine (1981). Both estimates include an additional 20% to account for mass outside the last planetary nebula.

Another way to constrain the mass is to ask what is the minimum needed to give the  $i$ th nebula the observed velocity. For a point mass this is the parabolic velocity  $v_i$  at closest approach  $r_i$  directed along our line of sight:

$$M_{\text{min}} = \frac{r_i v_i^2}{2G} \quad (6)$$

A distributed mass like M32 makes things more complicated since the planetary sees a varying mass through its orbit. Equation (6) is then not a lower limit to the total mass inside  $r_i$ , but it is a firm lower limit to the total mass of the galaxy. The highest  $M_{\text{min}}$  is from planetary M32-15:  $1.8 \times 10^8 M_{\odot}$ , only  $\sim 20\%$  of the most probable mass.

Most older mass estimates use assumptions which are suspect. Galaxies are not isothermal, and assuming they are (e.g., Poveda’s formula) will overestimate the mass. King model fits are difficult in any case, since the “core radius” tends to be suspiciously close to the size of the seeing disk, particularly for M32. When cores are resolved, they are poorly fitted by King models (Lauer 1985). Likewise, estimates based on nuclear velocity dispersions which are derived from a single-template star spectrum rather than a composite spectrum will overestimate the mass (Williams 1977).

#### IV. DISCUSSION

We have shown that the velocity dispersion tensor through the bulk of M32 is probably close to isotropic. How does this compare with observations of other ellipticals and prevailing

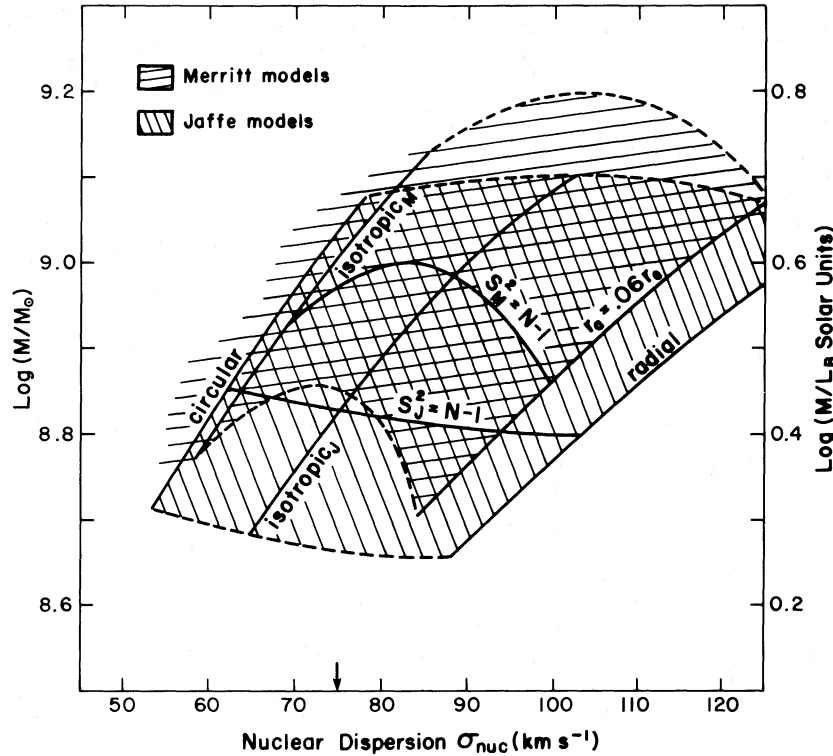


FIG. 5.—Mass and  $M/L_B$  vs. nuclear velocity dispersion. Planetary nebulae data favor values near the  $S_J^2 = N - 1$  and  $S_M^2 = N - 1$  curves for the Jaffe and de Vaucouleurs models, respectively. Masses for the de Vaucouleurs models are 30%–40% higher than for the Jaffe models. Dashed lines are 95% confidence limits. Merritt's de Vaucouleurs models do not have realistic dispersion profiles for cases where tangential dispersion dominates; thus, the lack of a boundary to the shading left of the isotropic  $M$  curve.

ideas of their structure? Unfortunately, there are virtually no dynamical data on the outer regions of other ellipticals. Dispersion profiles in the inner regions ( $r < r_e$ ) of many of the brighter E's are now available. They are flat near the core, and flat or slightly falling further out (e.g., Faber and Jackson 1976; Schechter and Gunn 1979; Davies and Illingworth 1983). The best data are from NGC 4472, and are quite consistent with an isotropic profile (Illingworth 1981; Jaffe 1983).

Most dissipationless galaxy collapse models predict that violent relaxation will produce isotropic cores, so the observations are perhaps not surprising. However, these same models predict the outer regions will have predominantly radial orbits. Within the model assumptions, our results for M32 can only be

reconciled with highly radial orbits if (a) observers have significantly underestimated the nuclear dispersion, or (b) the mass to light ratio increases with radius. The first possibility is unlikely, since the relevant biases tend to increase rather than decrease  $\sigma_{nuc}$ . However, an increasing  $M/L$  has been suspected of at least some ellipticals: Abell 2029 (Dressler 1979), IC 2082 (see Carter *et al.* 1981), the shell ellipticals studied by Hernquist and Quinn (1985), and *Einstein* X-ray data showing halos around many otherwise ordinary ellipticals (Forman, Jones, and Tucker 1985). A straightforward way of quantifying what is needed for M32 is to assume the density profile is the same as the mass profile, but with a larger scale. We experimented with such models following a Jaffe profile and estimate that  $M/L$

TABLE 5  
SUMMARY OF RECENT  $M/L$  ESTIMATES FOR M32

Method	Source	$M/L$ (uncorrected) <sup>a</sup>	$M/L_B$ <sup>b</sup>
Virial theorem on oblate spheroid	1	4.6 (core, $V$ band)	2.6
Modified virial theorem	2	3.6 ( $r < r_e$ , $B$ band)	3.9
Population synthesis model fit	3	3.8 (core, $B$ band)	3.8
Fitting Jaffe $\sigma(a)$ to PN data	This study		2.8
Fitting $r^{1/4} \sigma(a)$ to PN data	This study		3.7
Virial theorem on PN data	This study		0.7
Bahcall-Tremaine projected mass	This study		3.4

<sup>a</sup> Quoted from source.

<sup>b</sup> Scaled to our system by using  $\sigma_{nuc} = 75 \text{ km s}^{-1}$  and shifted to  $M/L_B$  by assuming  $B - V = 0.85$ .

SOURCES.—(1) Bendinelli, Parmeggiani, and Zavatti 1983. (2) Michard 1980. (3) Faber and French 1980.

must increase by close to an order of magnitude from core to outer halo before the planetary nebulae favor strongly radial orbits.

Is there evidence for increasing  $M/L$  in M32? One way to check is look at core versus global  $M/L$  estimates. If the dispersion tensor in the core is isotropic and isothermal, then a measure of the core  $M/L$  is

$$\frac{M}{L_{\text{core}}} = \frac{1.27 \times 10^{-7} \sigma_{\text{nuc}}^2 (\text{km s}^{-1}) 10^{0.4m_v}}{r_c (\text{pc})} \quad (7)$$

(King and Minkowski 1972), where  $r_c$  is the core radius from a King model fit, and we have converted Binney's (1982, eq. [19]) formula by using  $m_v$  magnitudes per square arc second central brightness. Although our method gives a global  $M/L$ , we have already used the nuclear dispersion and light profile, so that equation (7) does not give independent information. There are other problems with this method, beginning with the King model fit. The  $r^{1/4}$  model provides a better fit to the cores of ellipticals in general (de Vaucouleurs and Capaccioli 1979; Binney 1980; Schweizer 1979) and to M32 in particular (Wirth and Gallagher 1984; Schweizer 1979; Light, Danielson, and Schwarzschild 1974; de Vaucouleurs 1953). Resolving the core is another problem, since seeing will smear both a King model and an  $r^{1/4}$  profile into a King profile with a lower concentration index. Estimates of  $r_c$  have differed widely, from  $10''.2$  (de Vaucouleurs 1974) to less than  $0''.3$  by Light, Danielson, and Schwarzschild (1974). Smith (1935) used the Mount Wilson 2.5 m for a direct visual estimate in excellent seeing and found  $r_c < 0''.4$ . King and Minkowski (1972) quote a value of  $r_c = 2$  pc ( $= 0''.6$ ). Jenner (unpublished) used unpublished data from King to find  $r_c = 2''.3$ . Obviously, the core is unresolved. Another way to estimate a core  $M/L$  is by stellar population fits. Such studies have actually indicated an  $M/L$  decreasing with radius, in some cases.

de Vaucouleurs (1974, pp. 21, 23) quotes a mild  $M/L$  decrease from 5.4 in the core to 3.1 in the halo, based on a decreasing  $M/L$  model of Einasto. Faber and French (1980) find M dwarf enrichment and a high  $M/L$  in the nuclei of some galaxies, including M31. However, M32 shows no evidence for this. In fact, their population synthesis model fit for M32 gives a nuclear  $M/L_B$  of 3.8, in good agreement with our dynamical value for the galaxy as a whole. In the same paper, they find that M32 is best fit with an initial mass function exponent of zero, an unusually low value which is consistent with a low overall  $M/L$ . Michard's (1980)  $M/L_B$  of 3.9 inside  $r_e$  (after correcting to a  $\sigma_{\text{nuc}}$  of  $75 \text{ km s}^{-1}$ ) and the observed lack of a color gradient (Sharov and Lyutyj 1983) also indicate  $M/L$  changes little, if any, between the core and halo. We think a significantly decreasing  $M/L$  is unlikely, since the planetary nebula data would then favor a velocity ellipsoid which was significantly elongated in the azimuthal direction. This would be difficult to explain theoretically.

There are also theoretical arguments against a strongly increasing  $M/L$  with radius. M32 has almost certainly been affected by M31 (Keenan and Innanen 1975; King 1962). Any dark halo would probably have been tidally stripped. Absorption line strengths suggest M32 may originally have been  $\sim 1$  mag brighter (Faber 1973). Its light profile and the fact that it seems to follow the Faber-Jackson relation (Whitmore 1980) suggests that it has since relaxed to a state typical of E's. Any extended envelope would also exacerbate M32's already precarious dynamical friction problem (Tremaine 1976). As is,

it may soon be dragged into M31. It may be that M32/M31-type systems exist only because they do not have extended halos and the dynamical friction problems that go with them. Gerola, Carnevalli, and Salpeter (1983) argue that dwarf ellipticals may be (in M32's case, tidal) remnants from much larger systems and predict they would have little or no  $M/L$  gradients (note, however, that M32's central density is unusually high for dE's and their rationale may be less compelling).

A spherical system made up of highly radial orbits is also unstable to bar formation. Merritt and Aguilar (1985) have shown that at least 10%–15% of the kinetic energy must be in tangential motion for stability. This roughly corresponds to the  $r_a = 0.2$  model tested here. M32 is not strictly spherical and may even be as elongated as Merritt and Aguilar's resulting bars, if seen nearly pole on.

Finally, we will note that an  $M/L_B$  of 2–4 is comparable to that for globular clusters, even though M32's light profile and central velocity dispersion seem to put it at the low end of the class of giant ellipticals (Wirth and Gallagher 1984) which, in general have larger  $M/L$ 's, even in the inner region (Lauer 1985; Faber and Jackson 1976; Katz and Richstone 1985).

All of these results are consistent with the hypothesis that M32 is a tidal remnant which has lost most or all of any dark halo it once had and has since relaxed into a rotating mildly nonspherical shape with a roughly isotropic velocity ellipsoid.

## V. CONCLUSIONS

We have developed a procedure for testing the goodness of fit between small sets of radial velocities of individual objects and trial dispersion profiles. This method uses available nuclear velocity dispersions to provide spatial information. We have applied it to M32, idealized as a spherical system with constant  $M/L$  and find the following:

1. The dispersion tensor through the bulk of M32 is probably close to isotropic. This is true for reasonable models both with and without a strong central density singularity. If we have underestimated the random error in the velocities by less than a factor of 2, our results do not change significantly. A larger underestimate would favor more radial orbits, but we consider this very unlikely.
2. The rms dispersion of the planetaries is  $42 \text{ km s}^{-1}$ . This, compared to the nuclear dispersion of  $70\text{--}80 \text{ km s}^{-1}$ , suggests  $M/L$  does not increase strongly with radius.
3. The resulting mass is  $8.2(\pm 2) \times 10^8 M_{\odot}$ , and  $M/L_B$  is 3–4 in solar units.
4. The weighted average of the planetary nebulae velocities, corrected for rotation, gives a systemic velocity of  $-189 \pm 10 \text{ km s}^{-1}$ .

R. A. N. thanks Robin Ciardullo, Sandy Faber, Walter Jaffe, and especially Simon White for some good conversations and helpful criticisms. This work formed part of R. A. N.'s dissertation; R. A. N. thanks the Office of Academic Computing at UCLA for a continuing grant of computer resources. Part of this work was done while a summer research associate at the Space Telescope Science Institute. R. A. N. also thanks the staff of Steward Observatory, who assisted in the final preparation of this paper. Part of this work was supported under NSF grant AST-8352062.

## REFERENCES

- Bahcall, J., and Tremaine, S. 1981, *Ap. J.*, **244**, 805.  
 Bendinelli, O., Parmeggiani, G., and Zavatti, F. 1983, *Ap. Space Sci.*, **91**, 461.  
 Binney, J. 1980, *M.N.R.A.S.*, **190**, 873.  
 ———. 1982, *Ann. Rev. Astr. Ap.*, **20**, 399.  
 Carter, D., Efsthathiou, G., Ellis, R. S., Inglis, I., and Godwin, J. 1981, *M.N.R.A.S.*, **195**, 15p.  
 Davies, R. L., and Illingworth, G. 1983, *Ap. J.*, **266**, 516.  
 de Vaucouleurs, G. 1953, *M.N.R.A.S.*, **113**, 134.  
 ———. 1974, in *IAU Symposium 58, The Formation and Dynamics of Galaxies*, ed. J. R. Shakeshaft (Dordrecht: Reidel), p. 21.  
 de Vaucouleurs, G., and Capaccioli, M. 1979, *Ap. J. Suppl.*, **40**, 699.  
 de Vaucouleurs, G., de Vaucouleurs, A., and Corwin, H. 1976, *Second Reference Catalog of Bright Galaxies* (Austin: University of Texas Press) (RC2).  
 Dressler, A. 1979, *Ap. J.*, **231**, 659.  
 Faber, S. M. 1973, *Ap. J.*, **179**, 423.  
 Faber, S. M., and French, H. B. 1980, *Ap. J.*, **235**, 405.  
 Faber, S. M., and Jackson, R. E. 1976, *Ap. J.*, **204**, 668.  
 Ford, H. C., Jacoby, G., and Jenner, D. C. 1978, *Ap. J.*, **223**, 94.  
 Ford, H. C., and Jenner, D. C. 1975, *Ap. J.*, **202**, 365 (Paper II).  
 Forman, W., Jones, C., and Tucker, W. 1985, *Ap. J.*, **293**, 102.  
 Gerola, H., Carnevalli, P., and Salpeter, E. E. 1983, *Ap. J. (Letters)*, **268**, L75.  
 Gunn, J. E., and Griffin, R. F. 1979, *A.J.*, **84**, 752.  
 Heisler, J., Tremaine, S., and Bahcall, J. N. 1985, *Ap. J.*, **298**, 8.  
 Hernquist, L. E., and Quinn, P. J. 1985, in preparation.  
 Hesser, J. E., Harris, H. C., and van den Bergh, S., 1984, *Ap. J.*, **276**, 491.  
 Hubble, E. P. 1930, *Ap. J.*, **71**, 236.  
 Huchra, J., Stauffer, J., and van Speybroeck, L. 1982, *Ap. J. (Letters)*, **259**, L57.  
 Illingworth, G. 1981, in *The Structure and Evolution of Normal Galaxies*, ed. S. M. Fall and D. Lynden-Bell (Cambridge: Cambridge University Press), p. 27.  
 Jaffe, W. 1983, *M.N.R.A.S.*, **202**, 995.  
 Katz, N., and Richstone, D. O. 1985, *Ap. J.*, **296**, 331.  
 Keenan, D. W., and Innanen, K. A. 1975, *A.J.*, **80**, 290.  
 King, I. R. 1962, *A.J.*, **67**, 471.  
 King, I. R., and Minkowski, R. 1972, in *IAU Symposium 44, External Galaxies and QSOs*, ed. D. S. Evans (New York: Springer-Verlag), p. 87.  
 Lauer, T. R. 1985, *Ap. J.*, **292**, 104.  
 Lawrie, D. G., and Ford, H. C. 1982, *Ap. J.*, **156**, 112.  
 Light, E. S., Danielson, R. E., and Schwarzschild, M. 1974, *Ap. J.*, **194**, 257.  
 Lupton, R., Gunn, J., and Griffin, R. F. 1984, preprint.  
 Merritt, D. 1985, *A.J.*, **90**, 1027.  
 Merritt, D., and Aguilar, L. 1985, *M.N.R.A.S.*, **217**, 787.  
 Michard, R. 1980, *Astr. Ap.*, **91**, 122.  
 Newton, A. J., and Binney, J. 1984, *M.N.R.A.S.*, **210**, 711.  
 Nolthenius, R. A. 1984, Ph.D. thesis, University of California, Los Angeles.  
 Nolthenius, R., and Ford, H. C. 1986, in preparation.  
 Richstone, D. O., and Tremaine, S. 1984, *Ap. J.*, **286**, 27.  
 Saaf, A. F. 1968, *Ap. J.*, **154**, 483.  
 Schechter, P., and Gunn, J. E. 1979, *Ap. J.*, **229**, 472.  
 Schneider, S. E., Terzian, Y., Pergathofer, A., and Perinotto, M. 1983, *Ap. J. Suppl.*, **52**, 399.  
 Schweitzer, F. 1979, *Ap. J.*, **233**, 23.  
 Sharov, A. S., and Lyutyj, V. M. 1983, *Soviet Astr.*, **27**, p. 1.  
 Smith, S. 1935, *Ap. J.*, **82**, 192.  
 Tonry, J. L. 1983, *Ap. J.*, **266**, 58.  
 ———. 1984, *Ap. J. (Letters)*, **283**, L27.  
 Tremaine, S. D. 1976, *Ap. J.*, **203**, 345.  
 Trinchieri, G. 1985, preprint.  
 van den Bergh, S. 1969, *Ap. J. Suppl.*, **19**, 145.  
 Whitmore, B. C. 1980, *Ap. J.*, **242**, 53.  
 Williams, T. B. 1977, *Ap. J.*, **214**, 685.  
 Wirth, A., and Gallagher, J. S. 1984, *Ap. J.*, **282**, 85.

HOLLAND C. FORD: Space Telescope Science Institute, Homewood Campus, Baltimore, MD 21218

RICHARD NOLTHENIUS: Steward Observatory, University of Arizona, Tucson, AZ 85721